

Versatile system for the temperature-controlled preparation of oxide crystal surfaces

H. H. Pieper, C. Lammers, L. Tröger, S. Bahr, and M. Reichling^{a)}

Fachbereich Physik, Universität Osnabrück, Barbarastr. 7, 49076 Osnabrück, Germany

(Received 1 March 2012; accepted 27 April 2012; published online 21 May 2012)

We present a versatile system for the preparation of oxide crystal surfaces in the ultra-high vacuum (UHV) at temperatures up to 1300 K. Thermal treatment is accomplished by direct current heating of a tantalum foil in contact with the oxide sample. The sample temperature is measured by a thermocouple at a position close to the crystal and its reading is calibrated against the surface temperature determined by a second thermocouple temporarily attached to the surface. The design of the sample holder is based on a transferable plate originally developed for a commercial UHV scanning probe microscope. The system is, however, also suitable for the use with electron spectroscopy or electron diffraction based surface analytical techniques. We present results for the high-temperature preparation of CeO₂(111) surfaces with atomically flat terraces exhibiting perfect atomic order and cleanliness as revealed by non-contact atomic force microscopy (NC-AFM) imaging. NC-AFM imaging is, furthermore, used to demonstrate the temperature-controlled aggregation of gold atoms on the CeO₂(111) surface and their evaporation at high temperatures. © 2012 American Institute of Physics. [<http://dx.doi.org/10.1063/1.4717674>]

I. INTRODUCTION

Most surface science experiments are performed under ultra-high vacuum (UHV) conditions (residual gas pressure in the range of or below 10⁻¹⁰ mbar) to investigate clean surfaces with a well-defined structure and chemical composition. Many methods of UHV surface preparation require controlled heating of the crystal to remove contaminants,¹ to yield an equilibrium surface morphology,² a regular atomic structure^{3,4} or, for instance, to activate the diffusion of ad-particles to form cluster structures by sintering.^{5,6} Here, we focus on the preparation of surfaces of electrically insulating crystals. While some of them can easily be prepared by cleavage,⁷ others and specifically oxides are often most demanding in their preparation comprising steps of *ex situ* cutting and mechanical polishing and extended cycles of sputtering and annealing to high temperatures in UHV to obtain atomically well-ordered surfaces.⁸

Often, heating to high temperatures cannot be performed at the position of the measurement as the experimental equipment needs to be protected from thermal radiation. This is most relevant for scanning probe microscopy systems involving heat sensitive piezoelectric ceramics. Therefore, it is required to have a sample holder system allowing a transfer from a preparation stage to the experiment. A peculiarity arising from such a design is that electrical contacts have to be attached to the sample holder facilitating a precise measurement of the temperature with a thermocouple being as close as possible to the sample surface.

Numerous unique designs for sample transfer with different grabbing-mechanism were introduced including a bayonet coupling^{9,10} or a skewering of sample holders.^{11,12} The sample heating has to accommodate for certain

requirements such as highest temperature, maximum heating power, speed and accuracy of temperature ramps, precision in temperature measurement, or the possibility of LN₂ cooling of the sample.^{9,13-16} For heating, radiation and electron bombardment from a filament can be used,¹⁷ however, a resistive heating setup has been found to be more advantageous in certain situations even for generating temperatures above 1300 K.^{18,19} Here, we introduce a design tailored to the needs of oxide crystal preparation in the context of scanning probe microscopy. The requirements for the sample holder are in detail:

- (1) Compatibility with sample holder plates used for a commercial STM/AFM.
- (2) Transferability between the preparation stage and different instruments in the UHV system.
- (3) Suitability for mounting electrically insulating crystals with dimensions of about 8 × 2 × 0.5 mm³
- (4) Mechanical and thermal stability to allow for multiple preparation cycles repeated within a short time interval.
- (5) Sample preparation by cycles of Ar⁺ ion sputtering and annealing up to 1300 K.
- (6) Precise temperature measurement with a thermocouple.
- (7) Minimized power dissipation to reach the desired temperature.
- (8) Smooth up and down ramping of the temperature.
- (9) Avoiding the emission of electrons that could result in damaging or charging delicate electrically insulating samples.

To accomplish the preparation by sputtering and annealing and to allow for a facile transfer of the sample from the preparation stage to the experiments, there must be an adaptor where the sample holder can be securely fixed and manipulated during transfer and preparation. This adaptor must

- (1) allow transfer of the sample holder by a wobble stick,

^{a)} Author to whom correspondence should be addressed. Electronic mail: reichling@uos.de

- (2) be attached to a manipulator with XYZ and rotational degrees of freedom,
- (3) ensure that the axis of rotation is in the plane of the sample surface,
- (4) provide a slot for the sample holder with sliding contacts for heating and temperature measurement,
- (5) exhibit minimum degassing for typical heating powers,
- (6) allow electrical isolation of the sample holder, e.g. for flux measurements during Ar^+ ion sputtering or electron spectroscopy measurements.

As an additional requirement, the adapter should be suitable for inserting transfer plates carrying probes for STM and AFM measurements to put them into a position where they can be sputter cleaned.

II. SAMPLE HOLDER DESIGN

To accomplish all of these requirements, the sample holder is based on a plate design that has been introduced for a commercial UHV STM/AFM system (Omicron GmbH, Taunusstein, Germany). It allows for access to the sample surface over a large solid angle as it is required for scanning probe measurements as well as for electron spectroscopy or thermally programmed desorption measurements. Front view and exploded view of the sample holder assembly are shown in Figs. 1(a) and 1(b), respectively. The base plate carries the sample support made of Macor[®] ceramic accommodating samples with dimensions of about $8 \times 2 \times 0.5 \text{ mm}^3$. The sample support is fixed on the base plate by two M2 molybdenum screws one of them being electrically connected to one of the tantalum plates pressing the sample assembly onto the sample support and the base plate. The other tantalum plate is electrically isolated from the base plate. The sample is wrapped in a 0.015 mm thick tantalum foil that is used for direct current heating. The two tantalum plates fixing the sample act as electrical contact pads (see inset of Fig. 3(b)). The electrical resistance of the foil during heating is 0.5 to 1 Ω and it can withstand a dissipated power of about 15 W without excessive degradation. The desired temperatures can

be obtained by operating the heater with currents below 8 A at voltages below 4 V. The type K thermocouple assembly placed behind the sample is electrically insulated from the tantalum foil by a 0.15 mm thick alumina plate. This assembly is a chromel/alumel pair of sliding contacts anchored in notches of the sample support and bridged by a thin chromel wire. Hence, the temperature is measured at the point where the ceramic plate is pressed against the wire at the position of the alumel contact. The respective temperature reading is calibrated against the surface temperature by a procedure described in detail below. Heating of the sample by conductive heat transfer from a directly heated metal foil is chosen to minimize the heated volume and to avoid the emission of electrons present in radiative or electron bombardment heaters that could possibly damage the surface.^{20–22} Its proper operation requires a high degree of flatness of the sample back side, tantalum foil, and high rigidity of the ceramic plate to avoid the formation of any gaps between these components. Although, this implicates some technical effort, the temperature measurement by a thermocouple is preferred over the use of a pyrometer as results from the latter are often less accurate due to uncertainties in the sample (support) emissivity.

III. PREPARATION ADAPTOR DESIGN

For sample preparation, the sample holder is transferred to the preparation adaptor attached to a manipulator with XYZ and rotational degrees of freedom that is shown in Fig. 2(a). The purpose of the U-shaped connector (2) between the manipulator axis rod (1) and the adaptor (3) is to place the manipulator axis in the sample surface plane. Positioning the preparation adaptor at different positions by the manipulator facilitates a transfer of the sample holder from a storage carousel to the preparation adaptor and the STM/AFM or a load-lock adaptor by a wobble-stick catching the grip at the top of the sample holder base plate.

Details of the preparation adaptor are shown in Fig. 2(b). The slot for the sample holder (s1) has four sliding contacts (4,5) connected to insulated wires for the heater current and thermocouple wires connected to an electrical feedthrough at the top of the manipulator. The dimensions of the connector (2) are chosen to facilitate the transfer of samples, and probe transfer plates by a wobble stick in the slots (s1) and (s2) respectively. The adaptor block (3) made of stainless steel is electrically insulated from the connector and therefore from the chamber ground by four ceramic washers. This allows the measurement of the current through the base plate during sputter cleaning of the sample or during electron spectroscopic measurements. The front slot (s1) is equipped with a sliding contact (4) adapted to the left tantalum plate of the sample holder to conduct the heater current. This slot also provides thermocouple contacts (5) at the bottom. The wiring (not shown) of the preparation adaptor is loosely wound around the manipulator axis rod (1) granting the flexibility needed for the full rotation of 360°. The thickness of the cables is chosen to allow heating currents up to 20 A. Because currents typically applied are only a fraction of this value, a degassing of the wiring during the experiments can be excluded.

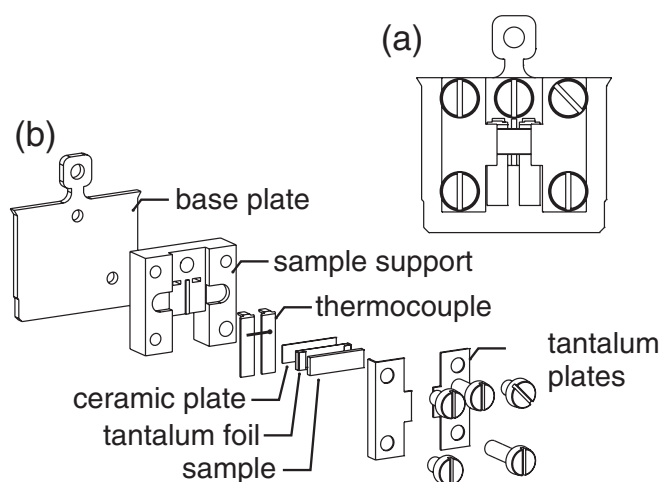


FIG. 1. Design of the sample holder assembly in front view (a) and exploded view (b).

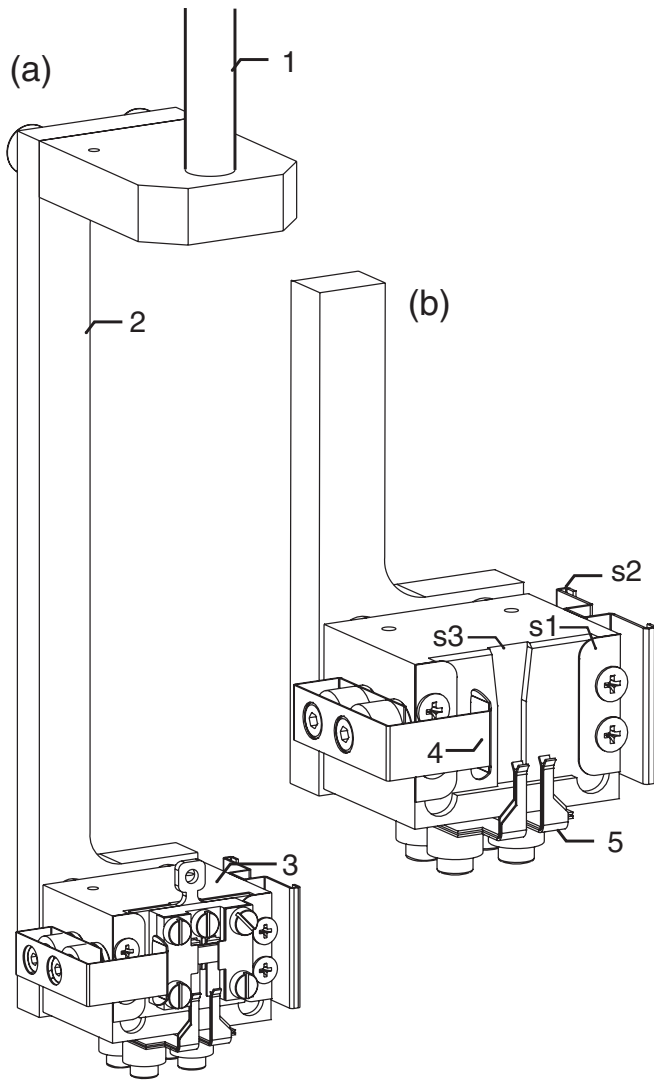


FIG. 2. Design of the preparation adaptor in overview with the sample holder inserted (a) and in detail with the sample holder removed (b). The numbered components are explained in the text.

For NC-AFM experiments, the preparation of the probes by Ar-sputtering is desirable. Therefore a mini slot (s3) is embedded in the center of the sample adaptor block behind the sample slot (s1). An alternative is placing the probe held by a transfer plate to an additional slot at the side of the adaptor block (s2).

IV. TEMPERATURE CALIBRATION AND SAMPLE HEATING

A benefit of the sample holder design presented here is the temperature readout by a thermocouple. However, it is mostly not feasible to place a thermocouple directly on the sample surface to measure the surface temperature T_s as the thermocouple would be an obstacle on the front side and could result in surface contamination. Therefore, the thermocouple is placed underneath the sample and measures a temperature T_{tc} that is generally not identical to the surface temperature. For calibration purpose, the surface temperature T_s is measured by a second thermocouple temporarily pressed onto the sample surface, as shown in the inset of Fig. 3(b). Positioning

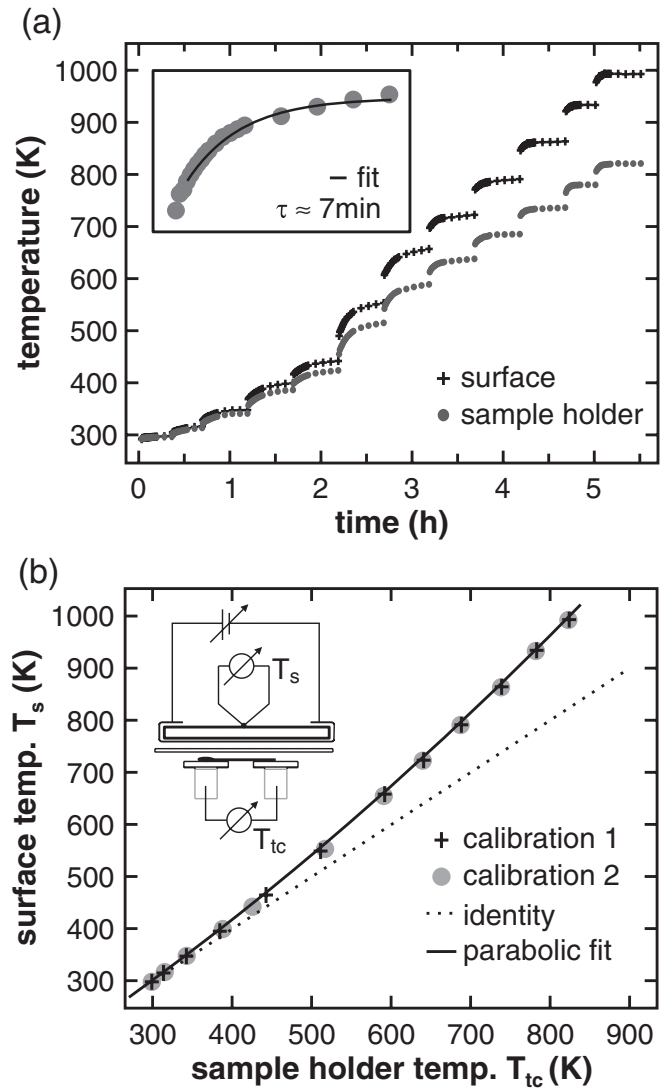


FIG. 3. (a) Surface temperature T_s and sample holder temperature T_{tc} as a function of time for step-wise increasing the heating power. The inset shows an exponential fit to the data for one step. (b) Surface temperature T_s and sample holder temperature T_{tc} as measured after thermal equilibration in each step plotted against each other. The inset shows a schematic representation of the calibration experiment. Note that gaps between the heater foil, ceramic plate, and thermocouple are drawn for better clarity of the figure but should be avoided in the heater assembly.

the permanent thermocouple below the sample and separating it from the heating tantalum foil by a thin ceramic plate ensures that the deviation between the temperatures T_s and T_{tc} is limited to a maximum of 20% of the surface temperature.

Figure 3(a) shows a calibration measurement performed with a silicon plate replacing the oxide sample. The surface temperature is increased from room temperature to 1000 K by stepwise increasing the heater current. Temperatures T_{tc} and T_s are plotted as a function of time. At each heating step, the temperatures T_{tc} and T_s rise from initial values T_i to final temperatures T_f following a function that can quite well be approximated by the exponential function

$$T(t) = T_f - (T_f - T_i) \exp(-t/\tau),$$

where τ is a time constant determined by the details of conductive and radiative heat transfer and the heat capacity of the

sample assembly. The inset in Fig. 3(a) shows an exemplary fit of the exponential function to measured T_{ic} values. The time constant is found to be roughly 7 min for all heating steps for both temperatures. The asymptotic values of T_{ic} and T_s after thermal equilibration for all heating steps are plotted against each other in Fig. 3(b). For increasing temperature, the values differ more and more from identity. To derive a calibration function, we perform a parabolic fit to the curve

$$T_s = a + b T_{ic} + c T_{ic}^2$$

yielding $a = 1.16$ K, $b = 0.876$ and $c = 4.06 \times 10^{-4}$ K $^{-1}$. As evident from Fig. 3(b), a second calibration measurement yields the same result within experimental error pointing to the excellent reproducibility of the calibration procedure. Considering the time constant to reach thermal equilibrium, it is found that optimum heating results are obtained by ramping the temperature with about 0.5 Ks $^{-1}$ and waiting for a time interval of several τ before performing an experiment at the desired temperature. However, for the interpretation of the respective experiment, the entire temperature history has to be regarded. For flashing the sample, a high peak temperature can rapidly be reached when applying a high heating power for a short period. In such a case, however, a precise surface temperature control is not possible unless considerable efforts in additionally calibrating the system for thermal transients are undertaken.

V. OXIDE SURFACE PREPARATION

To demonstrate the capabilities of the described system, we prepare a CeO₂(111) surface by sputter/annealing cycles and then deposit gold atoms on the surface with the substrate kept at room temperature. By subsequent controlled, step-wise heating of the sample, we observe processes of aggregation of gold atoms into nanoparticles and eventually the evaporation of gold from the clusters. The CeO₂(111) surface is initially prepared by some ten cycles of argon sputtering and subsequent annealing. The sputter parameters are 1.5 keV energy of the Ar⁺ ions, 5 min exposure time and a current of about 8 μ A through the sample holder. For annealing, the heating power is monotonically increased for about 30 min until a temperature of about 1300 K is reached. After keeping this value for a period of 15 min, the heating power is decreased for 30 min. This procedure results in an equilibrium surface morphology exhibiting atomically flat terraces with hexagonally shaped pits and protrusions as shown in Fig. 4(a) and described elsewhere in detail.²³ For this preparation, conditions have been chosen to obtain clean terraces that are well-ordered at the atomic scale²⁴ as revealed by NC-AFM images taken after the crystal has cooled down to room temperature (Fig. 4(b)) and only rarely vacancies²⁵ and other defects²⁶ or adsorbed water²⁷ are found.

In the second part of the experiment, gold is evaporated from the molybdenum crucible of an e-beam evaporator (EFM3, Omicron NanoTechnology GmbH, Taunusstein, Germany) to yield a surface coverage of about 0.15 ML. Figures 4(c)–4(f) represent exemplary measurements of the evolution of gold clusters in a series of post-deposition

annealing cycles. For each cycle, the temperature is increased by about 100 K compared to the previous one and the temperature is kept constant for one hour. As seen in Fig. 4(c), gold atoms nucleate into small clusters randomly distributed over terraces and step edges. An analysis of this and similar images yields that clusters have a narrow size distribution with a mean height corresponding to one or two atomic layers. Increasing the temperature results in Ostwald ripening and the cluster height increases to several nanometers as seen in Fig. 4(d). Upon further heating, the cluster density decreases and the gold atoms condense into aggregates solely nucleated at step edges and kink sites as it is evident from Fig. 4(e). Annealing at even higher temperatures results in the evaporation of metal and at 1245 K, the entire gold has desorbed from the surface, leaving the bare CeO₂(111) surface with the same morphology as Fig. 4(a). While details of such cluster manipulation experiments and their interpretation will be published elsewhere, here we summarize that our heating system allows a controlled preparation of oxide samples involving heating

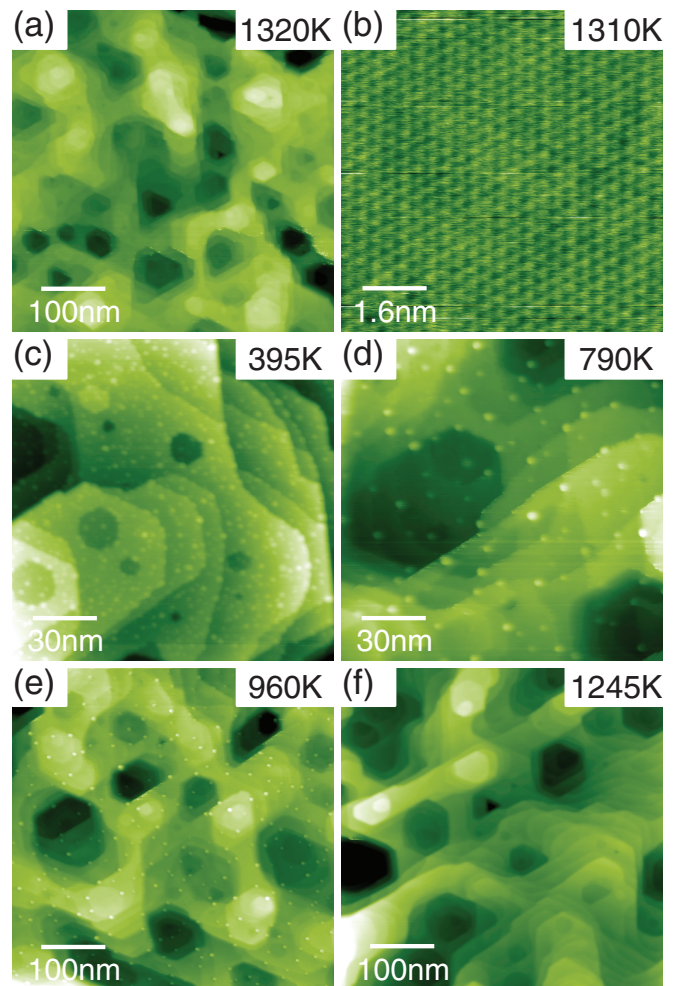


FIG. 4. (a) and (b) NC-AFM images of a stoichiometric CeO₂ surface after multiple cycles of Ar⁺ ion sputtering and annealing at temperatures up to 1300 K. A narrow band Fourier filter has been applied to the image of frame (b) to remove a spurious 50 Hz oscillation coupled into the signal detection path. (c) to (f) Images taken after deposition of 0.15 ML gold at room temperature and stepwise heating the sample to the temperatures shown in the upper right corner of the frames.

of the sample to temperatures up to 1300 K and a precise control of the surface temperature in experiments where the surface mobility of ad-particles is a crucial parameter.

ACKNOWLEDGMENTS

Support of this work by the Deutsche Forschungsgemeinschaft via the project RE 1186/12-1 is gratefully acknowledged.

- ¹P. A. Redhead, *Vacuum* **12**, 203 (1962).
- ²C. Misbah, O. Pierre-Louis, and Y. Saito, *Rev. Mod. Phys.* **82**, 981 (2010).
- ³G. Binnig, H. Rohrer, C. Gerber, and E. Weibel, *Phys. Rev. Lett.* **50**, 120 (1983).
- ⁴C. Barth and M. Reichling, *Nature (London)* **414**, 54 (2001).
- ⁵F. Loske, J. Lübke, J. Schütte, M. Reichling, and A. Kühnle, *Phys. Rev. B* **82**, 155428 (2010).
- ⁶M. C. R. Jensen, K. Venkataramani, S. Helveg, B. S. Clausen, M. Reichling, F. Besenbacher, and J. V. Lauritsen, *J. Phys. Chem. C* **112**, 16953 (2008).
- ⁷L. Tröger, J. Schütte, F. Ostendorf, A. Kühnle, and M. Reichling, *Rev. Sci. Instrum.* **80**, 063703 (2009).
- ⁸J. V. Lauritsen and M. Reichling, *J. Phys.: Condens. Matter* **22**, 263001 (2010).
- ⁹R. Raval, M. A. Harrison, D. A. King, and G. Caine, *J. Vac. Sci. Technol. A* **9**, 345 (1991).
- ¹⁰E. T. Krastev and R. G. Tobin, *J. Vac. Sci. Technol. A* **16**, 743 (1998).
- ¹¹N. J. Dinardo, J. E. Demuth, W. A. Thompson, and P. G. Ledermann, *Rev. Sci. Instrum.* **55**, 1492 (1984).
- ¹²H. J. Drouhin, M. Picard, and D. Paget, *Rev. Sci. Instrum.* **60**, 1167 (1989).
- ¹³C. M. Leitao, T. A. Gasche, G. Bonfait, O. Teodoro, and A. M. C. Moutinho, *Vacuum* **52**, 23 (1999).
- ¹⁴U. Leist, A. Winkler, J. Bussow, and K. Al-Shamery, *Rev. Sci. Instrum.* **74**, 4772 (2003).
- ¹⁵H. P. Marques, D. C. Alves, A. R. Canario, A. M. C. Moutinho, and O. Teodoro, *Rev. Sci. Instrum.* **78**, 035103 (2007).
- ¹⁶V. A. Bykov, B. K. Medvedev, S. A. Saunin, and D. Y. Sokolov, *Instrum. Exp. Tech.* **45**, 729 (2002).
- ¹⁷T. Mendus and A. Chambers, *J. Vac. Sci. Technol. B* **16**, 1258 (1998).
- ¹⁸C. A. Crider, G. Cisneros, P. Mark, and J. D. Levine, *J. Vac. Sci. Tech.* **13**, 1202 (1976).
- ¹⁹A. L. Helms, W. A. Schiedt, and S. L. Bernasek, *Rev. Sci. Instrum.* **59**, 1223 (1988).
- ²⁰R. Bennowitz, C. Günther, M. Reichling, E. Matthias, S. Vijayalakshmi, A. V. Barnes, and N. H. Tolk, *Appl. Phys. Lett.* **66**, 320 (1995).
- ²¹M. Reichling, R. M. Wilson, R. Bennowitz, R. T. Williams, S. Gogoll, E. Stenzel, and E. Matthias, *Surf. Sci.* **366**, 531 (1996).
- ²²R. Bennowitz, D. Smith, and M. Reichling, *Phys. Rev. B* **59**, 8237 (1999).
- ²³S. Torbrügge, M. Cranney, and M. Reichling, *Appl. Phys. Lett.* **93**, 073112 (2008).
- ²⁴S. Gritschneider and M. Reichling, *J. Phys. Chem. C* **112**, 2045 (2008).
- ²⁵S. Torbrügge, M. Reichling, A. Ishiyama, S. Morita, and O. Custance, *Phys. Rev. Lett.* **99**, 056101 (2007).
- ²⁶S. Gritschneider and M. Reichling, *Nanotechnology* **18**, 044024 (2007).
- ²⁷S. Gritschneider, Y. Iwasawa, and M. Reichling, *Nanotechnology* **18**, 044025 (2007).